

# Size-directed preparation of chitosan-carrageenan nanoparticles using dynamic light scattering for sustainable materials development

Carlo S. Emolaga <sup>a,b,\*</sup>, Lumen C. Milo <sup>b</sup>, Blessie A. Basilia <sup>a,c</sup>

<sup>a</sup> School of Graduate Studies, Mapúa University, 658 Muralla St., Intramuros, Manila 1002, Philippines

<sup>b</sup> DOST-Industrial Technology Development Institute, Department of Science and Technology, Gen. Santos Avenue, Brgy. Bicutan, Taguig City 1631, Philippines

<sup>c</sup> School of Chemical, Biological, and Materials Engineering and Sciences, Mapúa University, 658 Muralla St., Intramuros, Manila, 1002, Philippines

## ARTICLE INFO

**Keywords:**  
DLS  
Chitosan  
Carrageenan  
Nanoparticle

## ABSTRACT

The sustainable development of biopolymer-based nanoparticles using marine wastes and algal polysaccharides can significantly push the advancement of green chemistry and nanotechnology by reducing waste and using safer chemicals. This study uses a dynamic light scattering (DLS)-guided sequential approach for optimizing chitosan-carrageenan nanoparticles to produce a sustainable nanocarrier while minimizing reliance on the traditional trial-and-error methods. By adopting a systematic approach, this study ensures that the nanoparticles achieve the desired properties while minimizing waste in the production process. Chitosan is a biopolymer derived from crustacean waste while carrageenan can be extracted from seaweeds, an abundant marine resource. These raw materials can be used as encapsulating materials to address the limitations of bioactive compounds in drug delivery and other applications. The process involves selecting the appropriate chitosan molecular weight, carrageenan type, chitosan: carrageenan ratio, crosslinker type, and crosslinker concentration. The four-step formulation process identified a 5:1:1:3 ratio of low molecular weight chitosan,  $\kappa$ -carrageenan, sodium tripolyphosphate (STPP), and calcium chloride ( $\text{CaCl}_2$ ) as optimal, yielding nanoparticles with a hydrodynamic diameter of approximately 350 nm as measured by DLS. FTIR analysis confirmed successful chitosan-carrageenan nanoparticle formation, while AFM and TEM imaging revealed loosely aggregated particles with average sizes of ~150 nm in AFM and below 100 nm in TEM. This biopolymer-based nanoparticle can have applications in drug delivery, active packaging, and other related industries while supporting multiple Sustainable Development Goals (SDGs 2, 3, 6, and 12) and contributes to waste reduction and the advancement of eco-friendly materials science.

## 1. Introduction

Nanoparticles are auspicious materials with applications in various industries such as paper, water purification, catalysis, drug delivery, antibacterial products, food, and packaging industry [1]. Some metal-based nanoparticles in commercially available products, however, can be toxic to the human body and can harm the environment and the life of organisms therein [1]. The synthesis of many nanoparticles also requires high energy consumption, severe reaction conditions, and toxic chemicals, which can also generate toxic byproducts that can harm living beings and the environment [2]. In this context, biodegradable nanoparticles are needed to ensure safety across various industries [1].

As the demand for environmentally friendly and safe materials grows, there is a rising shift toward using nutraceuticals and other

bioactive agents in various applications. However, these compounds are prone to degradation and must be properly protected. One of the key applications of nanoparticles is encapsulating nutraceuticals and bioactive compounds to protect them from harsh and unfavorable conditions, such as pH fluctuations, light exposure, moisture, heat, chemical and biological degradation, and oxygen, throughout storage, processing, and use [3]. This process allows the bioactives to retain their functional properties throughout storage and enhance the shelf life and facilitate the incorporation of bioactives within different matrices [4,5]. Solid nanoparticles are categorized as either nanospheres or nanocapsules, defined as particles ranging from 10 to 1000 nm [6]. Food-grade biopolymers, like polysaccharides, are utilized in the encapsulation process as a coating agent to enhance the efficiency of bioactives. They have gained great popularity over synthetic polymers because of their

\* Corresponding author at: School of Graduate Studies, Mapúa University, 658 Muralla St., Intramuros, Manila 1002, Philippines.

E-mail addresses: [csemolaga@mymail.mapua.edu.ph](mailto:csemolaga@mymail.mapua.edu.ph) (C.S. Emolaga), [lcmilo@itdi.dost.gov.ph](mailto:lcmilo@itdi.dost.gov.ph) (L.C. Milo), [babasilia@mapua.edu.ph](mailto:babasilia@mapua.edu.ph) (B.A. Basilia).

immense functionalities and modifiability [4,7,8]. These biopolymers are generally recognized as safe (GRAS) materials, non-toxic, non-reactogenic, easily available at large scale and show remarkable biocompatibility and biodegradability [4].

One vast source of these polymeric biomaterials is the ocean. Marine polysaccharides are particularly valuable due to their inherent biological properties, biocompatibility and degradability, and diverse bioactivities, such as antitumor, antiviral, antioxidant, antimicrobial, anti-inflammatory, and immunomodulatory effects [9]. Among these, algal-derived polysaccharides like carrageenan have gained considerable attention as effective alternatives to conventional drug delivery systems [10]. Carrageenan also exhibits desirable properties, such as low cost, non-toxicity, biocompatibility, biodegradability, and low immunogenicity [11]. Another key approach to sustainable materials development involves the valorization of marine waste. Chitosan, a high-value biopolymer derived from crustacean waste, has found extensive applications across multiple industries, particularly in biomedical, food, and packaging sectors, due to its unique properties, including its role as a nanocarrier [12]. Rather than allowing marine waste to accumulate and contribute to environmental issues, its transformation into high-value biomaterials offers a sustainable pathway for resource utilization. The production of nanocarrier systems based on chitosan and carrageenan therefore exemplifies a promising strategy for advancing green and sustainable materials production.

Although chitosan and carrageenan are promising renewable materials for nanoparticle synthesis, their properties vary significantly based on molecular weight, type, and interaction ratios. Optimizing these parameters is crucial for achieving nanoparticles with desirable characteristics while ensuring the process remains sustainable.

One eco-friendly method to produce the nanoparticles is the ionic gelation method. One advantage of this method is that the formed nanoparticles are obtained spontaneously under mild control conditions without involving high temperatures, organic solvents, or sonication [13]. At lower concentrations of chitosan and carrageenan, nanoparticles can be formed using this method due to the electrostatic interaction between the negatively-charged carrageenan and the positively-charged chitosan. The physicochemical properties of these nanoparticles can be affected by factors such as 1) type of carrageenan, 2) the mass ratio of the polymers, 3) the solvent type used in the formulation, and 4) ionic strength of the medium [14], which must therefore be controlled.

Dynamic light scattering (DLS), also known as photon correlation spectroscopy or quasielastic light scattering, is the most common method used to examine the hydrodynamic size of particles in colloidal systems. It has developed into a quick and convenient tool for analyzing the size of noninteracting spherical colloids [15,16]. In this study, DLS was used as a quick guide to determine the factors to prepare chitosan-carrageenan nanoparticle. The factors that were considered include chitosan molecular weight (low MW and medium MW), carrageenan type (iota-carrageenan and kappa-carrageenan), chitosan:carrageenan ratio, crosslinker type (STPP, sodium citrate, and calcium chloride), and crosslinker ratio.

The use of biodegradable and renewable biopolymers such as chitosan and carrageenan is one way of promoting sustainable material development. The use of DLS-guided sequential approach, on the other hand, upholds green chemistry principles by minimizing trial-and-error in the preparation of nanoparticle. The chitosan-carrageenan nanoparticle also holds promise for sustainable drug delivery and active packaging, which supports circular economy principles in the packaging and healthcare industries. This study also supports sustainable practices and contribute to multiple facets of the sustainable development goals (SDGs), as chitosan-carrageenan nanoparticles can be used in drug delivery systems to enhance the efficacy and targeting of therapeutics for better health (SDG 3), controlled release of fertilizers in agriculture that can enhance food security by improving crop yields while minimizing environmental impact (SDG2), and water purification designs (due to

the inherent water purification properties of chitosan) that can remove pollutants from water, contributing to clean water initiatives (SDG 6). Both chitosan and carrageenan are also derived from natural sources making them renewable resources that promote sustainable practices and reduces reliance on synthetic polymers (SDG 12).

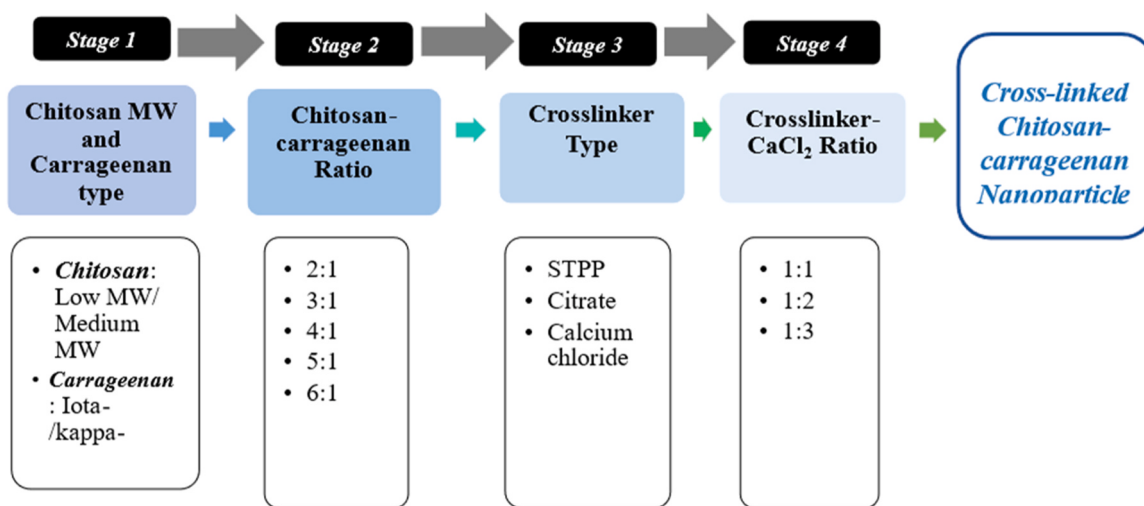
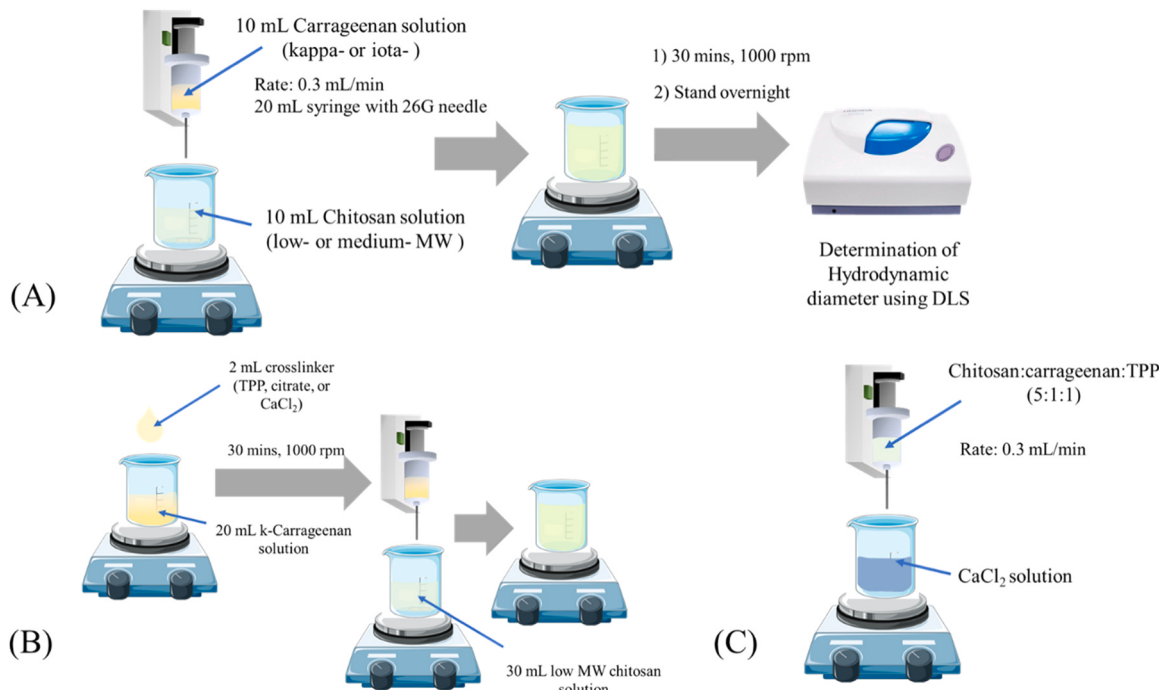
## 2. Materials and methods

Medium Molecular weight chitosan (75 % deacetylation; viscosity 407 cps) and Low Molecular Weight chitosan (76 % deacetylation, viscosity 101 cps), iota-carrageenan, and kappa-carrageenan were purchased from Sigma-Aldrich. Food-grade STPP (95.55 %) and Trisodium citrate dihydrate (99.8 %) were purchased from Dalkem Corporation, Philippines, while calcium chloride dihydrate (99.5 %) was purchased from Techno PharmaChem, India.

A 1 mg/mL solution of carrageenan was prepared by dissolving 0.25 g of carrageenan in 250 mL of deionized water, which was stirred overnight at 1000 rpm at room temperature. The pH of the solution was then adjusted to pH 4 using drops of 1 M HCl. Similarly, a 1 mg/mL chitosan solution was prepared by dissolving 0.25 g of chitosan in 1 % acetic acid, also stirred overnight at 1000 rpm at room temperature. This solution was filtered to remove any undissolved particles, and the pH was adjusted to pH 4 with drops of 1 M NaOH. For the crosslinkers—sodium tripolyphosphate (STPP), sodium citrate, and calcium chloride—a concentration of 10 mg/mL was achieved by dissolving 0.50 g of the crosslinker in 50 mL of deionized water, followed by stirring at 1000 rpm for 30 min.

Instead of relying on the traditional trial-and-error method, the preparation of the chitosan-carrageenan nanoparticles included four stages, summarized in Fig. 1. The first stage involved the use of different molecular weights of chitosan (low molecular weight or medium molecular weight) and different types of carrageenan (iota or kappa). A 1:1 (w/w) polyelectrolyte complex was prepared according to scheme shown in Fig. 2A, and the chitosan-carrageenan combination that gave the smallest hydrodynamic diameter was used for the second stage. In the second stage, chitosan and carrageenan solutions were mixed at different chitosan:carrageenan ratios (2:1, 3:1, 4:1, 5:1, 6:1). The chitosan:carrageenan ratio that gave the smallest hydrodynamic diameter was used for the third stage, which identified the suitable crosslinker (sodium citrate, STPP, calcium chloride) using the set-up shown in Fig. 2B. The crosslinker that gave the smallest hydrodynamic diameter was then used for the next stage. The ratio of the crosslinker and CaCl<sub>2</sub> (further crosslinking) was determined in the fourth stage, especially for the STPP crosslinker, using the set-up shown in Fig. 2C.

The hydrodynamic diameter of the samples at each processing stage was measured by dynamic light scattering (DLS) using a HORIBA nanoPartica SZ-100V2 Series particle size analyzer. Zeta potential measurements were conducted with a Malvern Zetasizer Lab Particle Size and Zeta Potential Analyzer (ZSU3105). The chemical composition of the synthesized nanoparticles was analyzed by Fourier Transform Infrared Spectroscopy (FTIR), with spectra acquired in the 4000–500 cm<sup>-1</sup> range using a PerkinElmer Spectrum Two FTIR spectrometer operated in attenuated total reflectance (ATR) mode. Atomic force microscopy (AFM) imaging was performed on an XE-100 (Park Systems) in tapping mode. A drop of diluted nanoparticle suspension was deposited onto a glass substrate, air-dried, and imaged under ambient conditions to assess particle morphology. Particle size and size distribution were determined using ImageJ software. Transmission electron microscopy (TEM) was utilized to examine the morphology, including shape, size, and internal structure of the nanoparticles. A drop of nanoparticle suspension was placed on a carbon-coated gold grid, air-dried, and imaged with a Jeol JEM-2100F TEM.

**Fig. 1.** Scheme for the preparation of chitosan-carrageenan nanoparticle.**Fig. 2.** Set-up for the nanoparticle formation of chitosan and carrageenan used for Stages 1 and 2 (A), Stage 3 (B), and Stage 4 (C).

### 3. Results and discussion

#### 3.1. Sustainable nanoparticle production scheme using dynamic light scattering

**Fig. 3A** shows that all chitosan-carrageenan combinations that use iota-carrageenan gave fibrous products, which could indicate that the resulting complexes formed extensive crosslinking. The formation of precipitate or fibrous aggregate in CH-low/iota-carrageenan and CH-med/iota-carrageenan could be due to the higher repulsion among the sulfate groups in iota-carrageenan compared to kappa-carrageenan, resulting in iota-carrageenan molecules to be less globular than kappa-carrageenan. As a result, the interactions between the cationic chitosan and anionic iota-carrageenan may be extensive enough, involving neighboring chitosan and iota-carrageenan molecules resulting in the formation of a visible fibrous precipitate.

According to Shchipunov et al. [17], the interaction involves the neutralization of charged groups through electrostatic interactions without causing the macromolecular chains to shrink into a globular form, as illustrated in case 2 of **Fig. 3B**. The rigid macromolecules act as a framework for a three-dimensional network, while the flexible ones serve as cross-linking junctions, which are more expansive than globules, with connections to a greater variety of macromolecules. Additionally, the arrangement of rigid macromolecular chains may contribute to the formation of these fibrillar structures. The low MW chitosan/kappa-carrageenan and medium MW chitosan/kappa-carrageenan combinations, on the other hand, gave slightly turbid suspensions, following Case 1 mechanism shown in **Fig. 3B**. The nanoparticles obtained from low molecular weight chitosan and kappa-carrageenan have a zeta potential of  $44.5 \pm 0.4$  mV, while the nanoparticles from medium molecular weight chitosan and kappa-carrageenan have a zeta potential of  $43.3 \pm 0.6$  mV. These values

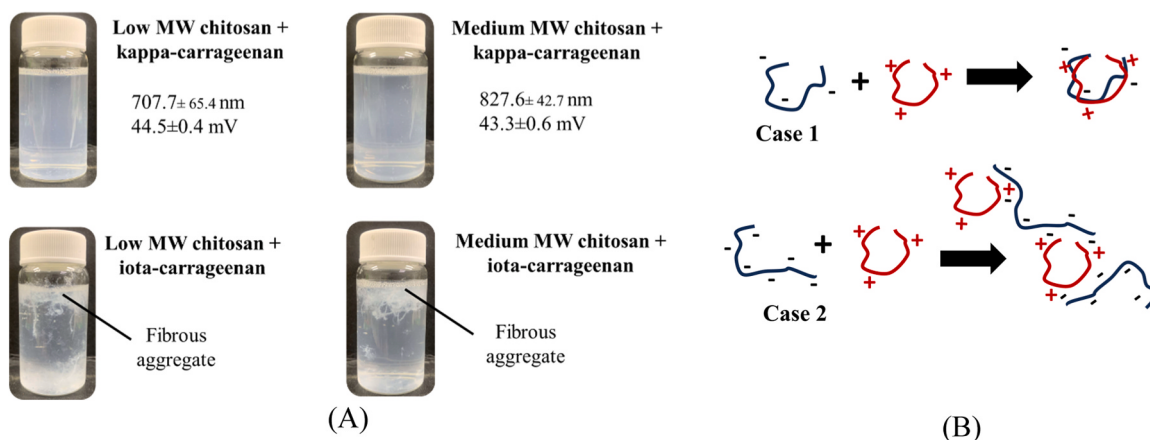


**Fig. 3.** Photos and hydrodynamic diameter and zeta potential of the nanoparticles of chitosan and carrageenan (A), and an illustration of possible mechanisms of chitosan-carrageenan polyelectrolyte complex formation (B).

confirm the source of stability of these two formulations.

This step showed that using kappa-carrageenan and low molecular weight chitosan leads to more stable nanoparticles than iota-carrageenan and medium molecular weight chitosan. This minimizes the need to include iota-carrageenan and medium molecular weight chitosan in the next steps, thus reducing material waste.

Based on the hydrodynamic diameter and zeta potential data in Fig. 3A, it is the combination of low MW chitosan and kappa-carrageenan that gave the lowest hydrodynamic diameter and higher zeta potential. Hence, this combination was used for the next stage, which involved different ratios of chitosan and carrageenan. Table 1 shows that 5:1 and 6:1 chitosan:carrageenan ratios are good candidates for the preparation of the nanocarrier. The observed decrease in size at higher chitosan ratios (5:1 and 6:1) can be attributed to the increased availability of cationic amino groups in chitosan, which enables more efficient and tighter ionic crosslinking with carrageenan's sulfate groups, leading to the formation of more compact and stable nanoparticles. Higher chitosan ratios are also expected to give higher net positive charge that contributes to electrostatic stabilization, reducing aggregation and yielding smaller hydrodynamic diameters. It can also be observed that the reduction in particle size from 5:1 (around 565 nm) to 6:1 (around 560 nm) is minimal. Since chitosan is the primary cost driver in the formulation, a 6:1 ratio requires more chitosan for minimal gain, increasing material costs unnecessarily. The 5:1 chitosan:carrageenan ratio therefore strikes the best balance between achieving significantly reduced particle size and ensuring practical production efficiency. The 5:1 ratio was also chosen because it would give a similar particle size but with a higher production yield than the 6:1 ratio [18]. This step ensures that the desired property is obtained while reducing the need for excess raw materials.

After selecting the chitosan molecular weight, carrageenan type, and chitosan-carrageenan ratio, the next step was the determination of the suitable crosslinker. Other than STPP, citrate/citric acid and  $\text{CaCl}_2$  were

also used as crosslinkers [19–23]. Rodrigues et al. [24] reported that cross-linking chitosan/carrageenan nanoparticles with tripolyphosphate resulted in a decrease in particle size and surface charge, as well as an increase in production yield and stability. They also found that incorporating TPP into the carrageenan dispersion before mixing it with chitosan significantly decreased the particle size and improved the yield. That is why in this step, the crosslinkers were added to kappa-carrageenan first before adding it to chitosan as shown in Fig. 2B. Table 2 shows that among the three crosslinkers, TPP gave the smallest particle size. Hence, it was the crosslinker used for the chitosan-carrageenan nanoparticle. TPP, as a polyanionic compound with multiple negative charges, facilitates the formation of strong and compact ionic crosslinks with the protonated amino groups of chitosan. In contrast, citrate, while also carrying multiple negative charges, has fewer available reactive sites than TPP, resulting in the formation of looser and less compact crosslinked networks. Calcium chloride ( $\text{CaCl}_2$ ) supplies divalent  $\text{Ca}^{2+}$  ions that engage in electrostatic interactions. However, these ions act primarily in a monodentate fashion, with each  $\text{Ca}^{2+}$  able to bridge at most two  $-\text{NH}_3^+$  groups, leading to weaker and less stable structures. Among the three crosslinkers, TPP produces a denser crosslinked matrix, yielding smaller and more stable nanoparticles.

A study by Yilmaz [25] showed that an additional treatment with  $\text{CaCl}_2$  after TPP crosslinking resulted in a further decrease in particle size. Table 3 shows the formulation and the particle size of the different particles, with sample 511–3 giving the smallest hydrodynamic diameter. This formulation also exhibited a zeta potential of  $42.35 \pm 0.45 \text{ mV}$ , indicating a stable dispersion.

Although the data suggest that further increasing the  $\text{Ca}^{2+}$  concentration could reduce the hydrodynamic diameter, the 511–3 formulation was identified as optimal to avoid excessive calcium levels that might destabilize the nanoparticles by over-neutralizing their surface charges, potentially causing aggregation or precipitation. This four-stage approach thus established a suitable formulation for the chitosan–carrageenan nanoparticles, consisting of a 5:1:1:3 ratio (low molecular weight chitosan:  $\kappa$ -carrageenan: STPP:  $\text{CaCl}_2$ ), which produced nanoparticles with a hydrodynamic diameter of approximately 350 nm.

Studies have shown that nanoparticles within the size range of approximately 40–400 nm are optimal for prolonging circulation time, improving tumor accumulation, and minimizing renal clearance,

**Table 1**  
Formulation and hydrodynamic diameter of the different ratios of low molecular weight chitosan and kappa-carrageenan.

	Chitosan: carrageenan Ratio				
	2:1	3:1	4:1	5:1	6:1
Volume of low MW chitosan (mL)	20	22.5	24	25	25.7
Volume of $\kappa$ -carrageenan (mL)	10	7.5	6	5	4.3
Hydrodynamic diameter (DLS), nm	655.2 $\pm$ 55.4	680.9 $\pm$ 82.1	679.1 $\pm$ 24.1	564.9 $\pm$ 72.8	558.7 $\pm$ 66.1

**Table 2**  
The hydrodynamic diameter of cross-linked 5:1 chitosan: carrageenan.

	Cross-linker		
	TPP	Citrate	$\text{CaCl}_2$
Hydrodynamic diameter (nm)	370.1 $\pm$ 94.2	503.4 $\pm$ 54.6	454.9 $\pm$ 22.3

**Table 3**

Formulation and resulting hydrodynamic diameter of chitosan:carrageenan:TPP particles with different amounts of  $\text{CaCl}_2$ .

Sample	511-1	511-2	511-3
Volume of $\text{CaCl}_2 \cdot 2\text{H}_2\text{O}$ (mL)	15.5	20.4	22.9
Volume of 5:1:1 chitosan:carrageenan:TPP (mL)	14.5	9.6	7.1
Total Volume (mL)	30	30	30
Hydrodynamic diameter (DLS), nm	488.2	419.9	354.9
	$\pm 139.2$	$\pm 73.5$	$\pm 56.3$

thereby enhancing their effectiveness in targeted drug delivery [26]. This indicates that the produced chitosan-carrageenan nanomaterial can be utilized for this type of application and other related applications.

### 3.2. Characterization of 5:1:1:3 (low molecular weight chitosan: kappa-carrageenan: STPP: $\text{CaCl}_2$ ) nanoparticle

Fig. 4 shows the FTIR spectra of the starting materials and the resulting nanoparticle. For chitosan, the characteristic peaks are shown in  $3288\text{ cm}^{-1}$  (N-H and O-H stretch),  $2873\text{ cm}^{-1}$  (C-H stretch),  $1648\text{ cm}^{-1}$  ( $\text{C=O}$  Amide I),  $1564\text{ cm}^{-1}$  (N-H+C-N Amide II),  $1313\text{ cm}^{-1}$  (N-H+C-N Amide III, CH), and  $1026\text{ cm}^{-1}$  (C-O-C, C-OH) [27,28]. For kappa-carrageenan, the characteristic peaks are found in  $3329\text{ cm}^{-1}$  (O-H stretch),  $2944\text{ cm}^{-1}$  (C-H stretch),  $1232\text{ cm}^{-1}$  (-S=O asymmetric vibration), around  $920\text{ cm}^{-1}$  (C-O vibration of 3,6 anhydrogalactose), and  $844\text{ cm}^{-1}$  (secondary axial sulfate group at C-4 of the 1,3-linked  $\beta$ D-galactose) [29].

TPP shows two intense bands at around  $1140\text{ cm}^{-1}$  and  $890\text{ cm}^{-1}$  due to P = O and P-O along with P-O-P, which often overlaps with the sulfate bands of kappa-carrageenan and the carbohydrate bands [24]. The new absorption band obtained after the complexation of chitosan and carrageenan appears at  $1529\text{ cm}^{-1}$  due to  $\text{NH}_3^+$ , which is absent in both chitosan and carrageenan. The typical bands of the sulfate group of carrageenan at  $1235\text{ cm}^{-1}$  and the galactose-4-sulfate at  $848\text{ cm}^{-1}$  are also seen in the spectrum of the nanoparticles. These indicate the formation of the nanoparticles from the complexation of chitosan and carrageenan [18].

The AFM images and size distribution of the 5:1:1:3 (low molecular weight chitosan: kappa-carrageenan: STPP:  $\text{CaCl}_2$ ) nanoparticle in Fig. 5 showed particle sizes of average particle size less than 200 nm. The image in Fig. 5A shows a high-density distribution of nearly spherical or semi-spherical nanoparticles in a clustered manner. This was when

several drops of the dispersion was applied on the glass and allowed to dry. When sonication was applied, the particles were more dispersed (Fig. 5B), which also allowed better determination of size distribution (Fig. 5C), showing majority of the particles in the 150 nm range. This result was further verified by the TEM images of the nanoparticles shown in Fig. 6. Fig. 6A shows that the individual particles are spherical to slightly oval, mostly less than 100 nm in diameter, but grouped into clusters spanning several hundred nanometers.

The observed loose aggregation pattern aligns with a balance between attractive electrostatic forces from polyelectrolyte complexation and repulsive forces from surface charges. As shown in Fig. 6B, spherical particles with diameters below 100 nm were evident. The complementary AFM and TEM analyses therefore confirmed the successful synthesis of chitosan-carrageenan nanoparticles exhibiting spherical morphology and nanoscale dimensions. It also displayed a tendency to loosely aggregate, which can be observed in polyelectrolyte complexes formed through ionic gelation.

In summary, the DLS-guided chitosan-carrageenan nanoparticles developed in this study exhibited a hydrodynamic diameter of approximately 350 nm by DLS, an average particle size of around 150 nm in AFM images, and sub-100 nm sizes in TEM analysis. These findings align well with previous reports indicating that chitosan/carrageenan nanoparticles typically range from 150 to 650 nm with positive zeta potentials under various preparation conditions [18,24]. The observed size variations across characterization techniques are consistent with differences in measurement principles, with DLS capturing hydrated particle size and AFM/TEM providing insights into dried or immobilized particles. Similar to the work of Klein et al. [30], the present results underscore the critical role of preparation conditions in tuning nanoparticle size and stability. Together, these findings reinforce the potential of chitosan-carrageenan nanoparticles as biocompatible carriers for drug delivery and other related applications.

Upscaling of this technology is expected to exert minimal pressure on chitosan production. Globally, approximately 8 million tons of crustacean shell waste are generated each year from crabs, shrimp, and lobsters [31]. This waste is often discarded or landfilled, contributing to ecosystem disruptions [31,32]. Valorizing this shell waste to produce chitosan aligns with sustainability objectives and supports applications in agriculture, biomedicine, and the food industry [32,33]. On average, about 20 % of crustacean shell waste can be converted into chitosan [34], equating to a potential annual production of 1.6 million tons of chitosan from the global shell waste stream. Even assuming that only 1 % of this potential is realized, approximately 16,000 tons of chitosan

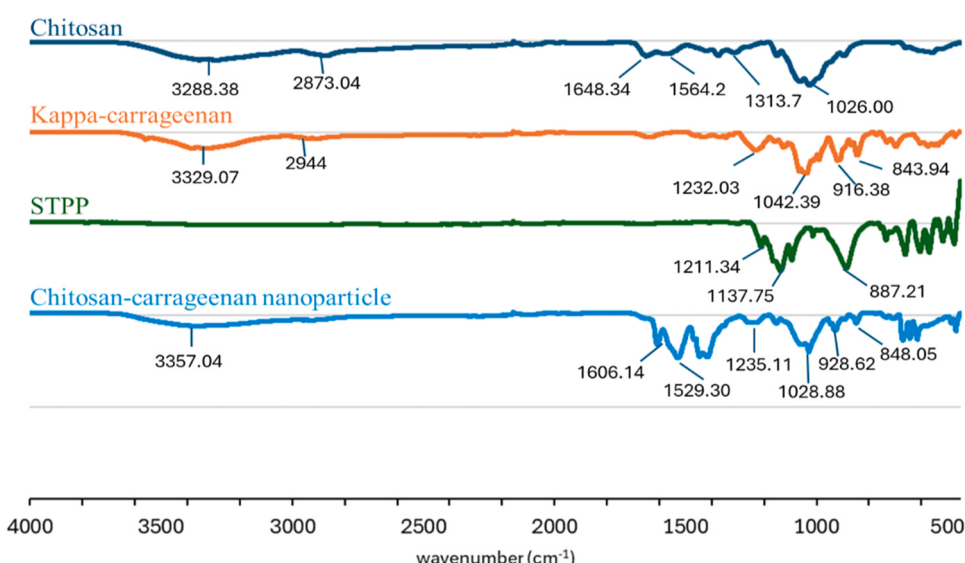
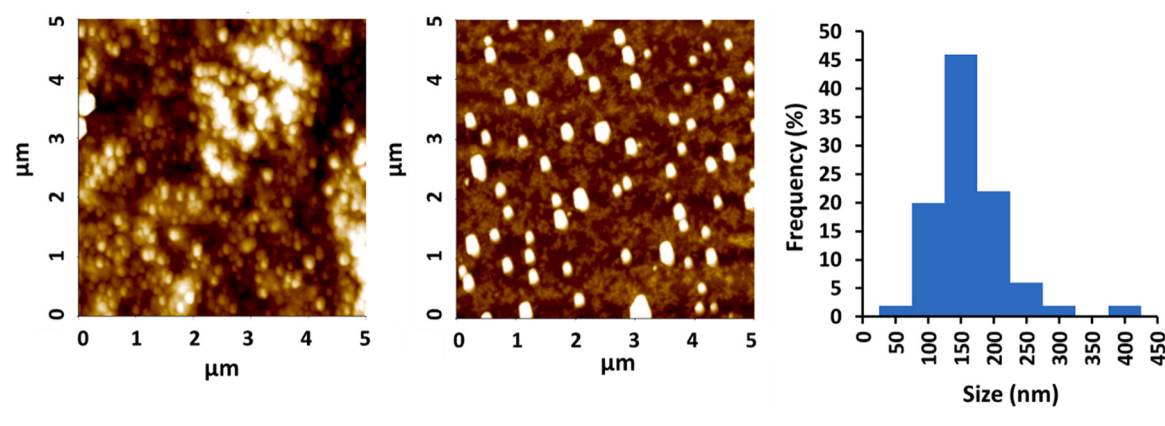
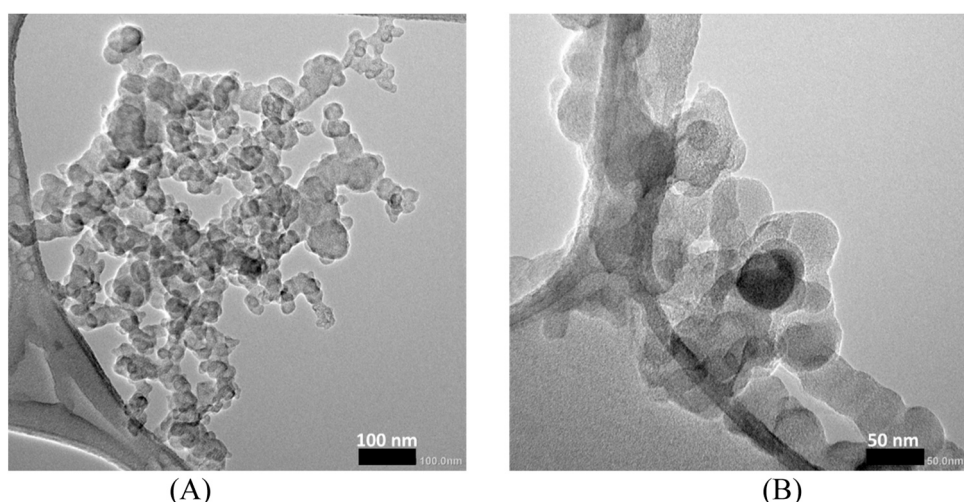


Fig. 4. FTIR spectra of the starting materials and the nanoparticle.



**Fig. 5.** AFM image of 5:1:1:3 chitosan:carageenan:TPP:CaCl<sub>2</sub> nanoparticles, showing the clustered particles (A), separated particles after sonication (B), and particle size distribution (C) with average size = 188 ± 54 nm (N = 50).



**Fig. 6.** TEM images of the nanoparticles at 50,000 x magnification (A), and 100,000 x magnification (B), showing spherical or semispherical particles with sizes less than 100 nm.

would still be produced each year. The nanoparticle formulation developed in this study (5:1:1:3), will require 50 kg of chitosan per month for a 100 kg of nanoparticles production per month. This would need 600 kg of chitosan annually per production site. Scaling up to 50 production sites would require 30,000 kg/year of chitosan—representing only about 0.2 % of the estimated annual chitosan production from crustacean waste. Therefore, expanding this nanoparticle formulation technology would exert minimal pressure on chitosan supply or crustacean harvests, particularly when waste shells are effectively utilized.

This study therefore confirms the use of biodegradable and renewable biopolymers such as chitosan and carageenan in a DLS-guided preparation of nanoparticles as a sustainable material development scheme.

#### 4. Conclusion

An environmentally responsible production of biodegradable nanoparticles was established using a dynamic light scattering (DLS)-guided protocol. A chitosan: carageenan nanoparticle was produced from low molecular weight chitosan and kappa-carageenan using STPP as crosslinker and CaCl<sub>2</sub> as additional crosslinking agent. Using particle size as the guide/basis for the preparation of the nanoparticle, the

sequential process was able to identify the appropriate molecular weight, carageenan type, chitosan; carageenan ratio, crosslinker type, and crosslinker ratio to reduce the initial hydrodynamic diameter of low molecular weight chitosan: kappa-carageenan from around 700 nm to around 350 nm. FTIR analysis confirmed successful chitosan–carageenan nanoparticle formation, while AFM and TEM imaging revealed loosely aggregated particles with average sizes of ~150 nm in AFM and below 100 nm in TEM. The final formulation of the nanoparticle is 5:1:1:3 low molecular weight chitosan: kappa-carageenan: STPP: CaCl<sub>2</sub>. Determining the correct parameters does not only ensure that the nanoparticles have the desired properties but also minimizes waste in the production method. This study therefore confirms the use of biodegradable and renewable biopolymers such as chitosan and carageenan in a DLS-guided preparation of nanoparticles for sustainable material development in the biomedical and other related industries.

#### CRediT authorship contribution statement

**Blessie A. Basilia:** Writing – review & editing, Validation, Supervision, Funding acquisition, Formal analysis, Conceptualization. **Lumen C. Milo:** Writing – review & editing, Validation, Investigation, Conceptualization. **Carlo S. Emolaga:** Writing – original draft,

Methodology, Investigation, Formal analysis, Conceptualization.

## Declaration of Competing Interest

The authors declare the following financial interests/personal relationships which may be considered as potential competing interests: Blessie A. Basilia reports financial support was provided by Royal Academy of Engineering UK. If there are other authors, they declare that they have no known competing financial interests or personal relationships that could have appeared to influence the work reported in this paper.

## Acknowledgments

This research is supported by the Royal Academy of Engineering UK, under the scheme on Engineering Skills Where They are Most Needed – Impact Grants Call 2021/23. CEmolaga is also thankful to Dr. Bryan Paul Bulatao of the National Institutes of Health of the University of the Philippines Manila for the technical help.

## Data availability

Data will be made available on request.

## References

- [1] A. Vodyashkin, P. Kezimana, A. Vetcher, Y. Stanishevskiy, Biopolymeric nanoparticles—Multifunctional materials of the future, *Polymers* 14 (2022) 2287, <https://doi.org/10.3390/polym14112287>.
- [2] T. Shafiq, M. Uzair, M. Iqbal, M. Zafar, S. Hussain, S. Shah, Green synthesis of metallic nanoparticles and their potential in bio-medical applications, *Nano Biomed. Eng.* 13 (2021) 191–206, <https://doi.org/10.5101/nbe.v13i2.p191-206>.
- [3] L. Rashidi, Different nano-delivery systems for delivery of nutraceuticals, *Food Biosci.* 43 (2021) 101258, <https://doi.org/10.1016/j.fbio.2021.101258>.
- [4] A. Karim, A. Rehman, J. Feng, A. Noreen, E. Assadpour, M. Kharazmi, Z. Lianfu, S. Jafari, Alginate-based nanocarriers for the delivery and controlled-release of bioactive compounds, *Adv. Coll. Int. Sci.* 307 (2022) 102744, <https://doi.org/10.1016/j.cis.2022.102744>.
- [5] Y. Gao, Y. Wu, Recent advances of chitosan-based nanoparticles for biomedical and biotechnological applications, *Int. J. Biol. Macromol.* 203 (2022) 379–388, <https://doi.org/10.1016/j.ijbiomac.2022.01.162>.
- [6] A. Lima, T. Gratieri, M. Cunha-Filho, G. Gelfuso, Polymeric nanocapsules: a review on design and production methods for pharmaceutical purpose, *Methods* 199 (2022) 54–66, <https://doi.org/10.1016/j.jymeth.2021.07.009>.
- [7] S. Akbari-Alavijeh, R. Shaddel, S. Jafari, Encapsulation of food bioactives and nutraceuticals by various chitosan-based nanocarriers, *Food Hydrocoll.* 105 (2020) 105774, <https://doi.org/10.1016/j.foodhyd.2020.105774>.
- [8] G. Maleki, E. Woltering, M. Mozafari, Applications of chitosan-based carrier as an encapsulating agent in food industry, *Trends Food Sci. Technol.* 120 (2022) 88–99, <https://doi.org/10.1016/j.tifs.2022.01.001>.
- [9] H. Geng, M. Chen, C. Guo, W. Wang, D. Chen, Marine polysaccharides: biological activities and applications in drug delivery systems, *Carbohydr. Res.* 538 (2024) 109071, <https://doi.org/10.1016/j.carres.2024.109071>.
- [10] N. Ramadan, Youssef, A. Alshishtawy, F. Elshikh, O. Newir, N. Abdelazeem, N. Ma'ruf, H. Shouman, S. Ali, M. El-Sheekh, Marine algal polysaccharides for drug delivery applications: a review, *Int. J. Biol. Macromol.* 295 (2025) 139551, <https://doi.org/10.1016/j.ijbiomac.2025.139551>.
- [11] Y. Dong, Z. Wei, C. Xue, Recent advances in carrageenan-based delivery systems for bioactive ingredients: a review, *Trends Food Sci. Technol.* 112 (2021) 348–361, <https://doi.org/10.1016/j.tifs.2021.04.012>.
- [12] Y. Yang, M. Aghbashlo, V. Gupta, H. Amiri, J. Pan, M. Tabatabaei, A. Rajaei, Chitosan nanocarriers containing essential oils as a green strategy to improve the functional properties of chitosan: a review, *Int. J. Biol. Macromol.* 236 (2023) 123954, <https://doi.org/10.1016/j.ijbiomac.2023.123954>.
- [13] M. Di Santo, C. D'Antoni, A. Rubio, A. Alaimo, O. Perez, Chitosan-tripolyphosphate nanoparticles designed to encapsulate polyphenolic compounds for biomedical and pharmaceutical applications – A review, *Biomed. Pharm.* 142 (2021) 111970, <https://doi.org/10.1016/j.bioph.2021.111970>.
- [14] A. Čirić, D. Krajišnik, B. Čalija, L. Đekić, Biocompatible non-covalent complexes of chitosan and different polymers: characteristics and application in drug delivery, *Arh. Farm* 70 (2020) 173–197, <https://doi.org/10.5937/arhfarm2004173Q>.
- [15] M. Tosi, A. Ramos, B. Esposto, S. Jafari, S. Dynamic light scattering (DLS) of nanoencapsulated food ingredients, in: S. Jafari (Ed.), *Characterization of Nanoencapsulated Food Ingredients*, Elsevier Inc, 2020, pp. 191–211, <https://doi.org/10.1016/B978-0-12-815667-4.00006-7>.
- [16] P. Hassan, S. Rana, G. Verma, Making sense of Brownian motion: colloid characterization by dynamic light scattering, *Langmuir* 31 (2015) 3–12. (<https://pubs.acs.org/doi/10.1021/la501789z>).
- [17] Y. Shchipunov, I. Postnova, Water-soluble polyelectrolyte complexes of oppositely charged polysaccharides, *Compos. Interfaces* 16 (2009) 251–279, <https://doi.org/10.1163/156855409X447093>.
- [18] A. Grenha, M. Gomes, M. Rodrigues, V. Santo, J. Mano, N. Neves, R. Reis, Development of new chitosan/carrageenan nanoparticles for drug delivery applications, *J. Biomed. Mater. Res.* 92 (2010) 1265–1272, <https://doi.org/10.1002/jbm.a.32466>.
- [19] M. Taghizadeh, H. Ashassi-Sorkhabi, R. Afkari, A. Kazempour, Cross-linked chitosan in nano and bead scales as drug carriers for betamethasone and tetracycline, *Int. J. Biol. Macromol.* 131 (2019) 581–588, <https://doi.org/10.1016/j.ijbiomac.2019.03.094>.
- [20] V. Rana, K. Babita, D. Goyal, A. Tiwary, Sodium citrate cross-linked chitosan films: optimization as substitute for human/rat/rabbit epidermal sheets, *J. Pharm. Pharm. Sci.* 8 (2005) 10–17.
- [21] B. Agu, P. Benabolo, V. Mesias, D. Penalosa, Jr, Synthesis and characterization of a chitosan-based citric acid-crosslinked encapsulant system, *J. Chil. Chem. Soc.* 64 (2019) 4610–4612.
- [22] M. Bagheri, H. Younesi, S. Hajati, S. Borghei, Application of chitosan-citric acid nanoparticles for removal of chromium (VI), *Int. J. Biol. Macromol.* 80 (2015) 431–444, <https://doi.org/10.1016/j.ijbiomac.2015.07.022>.
- [23] S. Kalliola, E. Repo, V. Srivastava, J. Heiskanen, J. Sirviö, H. Liimatainen, M. Sillanpää, The pH sensitive properties of carboxymethyl chitosan nanoparticles cross-linked with calcium ions, *Colloids Surf. B Biointerfaces* 153 (2017) 229–236, <https://doi.org/10.1016/j.colsurfb.2017.02.025>.
- [24] S. Rodrigues, A. Costa, R. Da, A. Grenha, Chitosan/carrageenan nanoparticles: effect of cross-linking with tripolyphosphate and charge ratios, *Carbohydr. Polym.* 89 (2012) 282–289, <https://doi.org/10.1016/j.carbpol.2012.03.010>.
- [25] H. Yilmaz, Preparation and characterization of chitosan- $\kappa$ -carrageenan based polymeric nanoparticles for gemcitabine delivery, *Erzincan Üniv. Fen. Bilim. Enst. Derg.* 15 (2022) 636–648.
- [26] M. Subhan, S. Yalamarty, N. Filipczak, F. Parveen, V. Torchilin, Recent advances in tumor targeting via EPR effect for cancer treatment, *J. Pers. Med.* 11 (2021) 571, <https://doi.org/10.3390/jpm11060571>.
- [27] L. Yakovishin, E. Tkachenko, Y. Tolstenko, E. Korzh, Development and IR spectroscopic analysis of composite material based on poly(Methyl Methacrylate) and chitosan, *Mater. Sci. Forum* 1065 (2022) 145–154, <https://doi.org/10.4028/p-5xpcm8>.
- [28] C. Branca, G. D'Angelo, C. Crupi, K. Khouzami, S. Rifici, G. Ruello, U. Wanderlingh, Role of the OH and NH vibrational groups in polysaccharide-nanocomposite interactions: a FTIR-ATR study on chitosan and chitosan/clay films, *Polymer* 99 (2016) 614–622.
- [29] A. Kravchenko, S. Anastyuk, V. Glazunov, E. Sokolova, V. Isakov, I. Yermak, Structural characteristics of carrageenans of red alga *Mastocarpus pacificus* from sea of Japan, *Carbohydr. Polym.* 229 (2020), <https://doi.org/10.1016/j.carbpol.2019.115518>.
- [30] R. Klein, D. de Almeida, A. de Oliveira, E. Bonafé, J. Monteiro, R. Sabino, A. Martins, Iota-carrageenan/chitosan nanoparticles via coacervation: achieving stability for tiny particles, *Nanomaterials* 15 (3) (2025), <https://doi.org/10.3390/nano15030161>.
- [31] N. Topić Popović, V. Lorencin, I. Strunjak-Perović, R. Čož-Rakovac, Shell waste management and utilization: mitigating organic pollution and enhancing sustainability, *Appl. Sci.* 13 (623) (2023), <https://doi.org/10.3390/app13010623>.
- [32] J.L. Vidal, T. Jin, E. Lam, F. Kerton, A. Moores, Blue is the new green: valorization of crustacean waste, *Curr. Res. Green. Sustain. Chem.* 5 (2022) 100330, <https://doi.org/10.1016/j.crgsc.2022.100330>.
- [33] S. Ngasotter, K. Xavier, M. Meitei, D. Waikhom, Madhulika, J. Pathak, S. Singh, Crustacean shell waste derived chitin and chitin nanomaterials for application in agriculture, food, and health – A review, *Carbohydr. Polym.* 16 (2023), <https://doi.org/10.1016/j.carpta.2023.100349>.
- [34] N. Nerdy, P. Lestari, D. Simorangkir, V. Auliansyah, F. Yusuf, T. Bakri, Comparison of Chitosan from carb shell waste and shrimp shell waste as natural adsorbent against heavy metals and dyes, *Int. J. Appl. Pharm.* 14 (2022) 181–185, <https://doi.org/10.22159/ijap.2022v14i2.43560>.